Integrated Geophysical and Hydrochemical Assessment of Groundwater Quality Near Urban Dumpsites in Port Harcourt, Nigeria

Celestine Gwunmitop Idaso, Prof. I. Tamunobereton-ari, Prof. A. R. C. Amakiri
Department of Physics, Faculty of Science,
Rivers State University, Nkpolu-Orowokwo,
Port Harcourt, Nigeria
https://doi.org/10.56201/ijgem.vol.12.no10.2026.pg277.294

Abstract
Open dumpsites may affect groundwater quality where permeable overburden permits surface-derived solutes to enter aquifer materials. This study integrated vertical electrical sounding (VES), electrical resistivity tomography (ERT), and borehole hydrochemical analysis at Eliozu, Rumuolumeni, and Iwofe in Port Harcourt, Nigeria. Seventeen VES stations and thirteen ERT profiles characterised subsurface resistivity structure and geoelectric protective capacity, while six borehole samples were analysed for physicochemical, microbial, heavy-metal, groundwater-quality-index (GQI), and hydrochemical-facies indicators. Conductive anomalies occurred at shallow to intermediate depths, including intervals extending to 33.40 m at Iwofe. Longitudinal conductance ranged from 0.001877 to 0.023766 S, placing all VES points in the poor class of the adopted protective-capacity rating. Reported GQI values were 126.72, 163.71, and 198.88 for the near-dumpsite boreholes and 35.94, 36.18, and 36.35 for the control boreholes. Higher reported phosphate, nitrate, iron, lead, and cadmium concentrations at near-dumpsite locations, together with an alkali–chloride facies tendency, are consistent with poorer measured groundwater quality. The results from the integrated geophysical and hydrochemical investigation of shallow aquifers around Eliozu, Rumuolumeni and Iwofe, demonstrate that groundwater within the dumpsite impacted zones has been affected by leachate infiltration.

Keywords: *Electrical resistivity tomography; groundwater quality index; hydrochemical facies; leachate; vertical electrical sounding*

1. Introduction

Municipal solid waste disposal remains a persistent groundwater-protection concern in rapidly urbanising parts of the Niger Delta. In Port Harcourt, open dumpsites commonly occupy abandoned borrow pits and other unengineered depressions. These sites generally lack liners, leachate-collection systems, and other barriers that would restrict contaminant release. Rainfall infiltrating mixed municipal waste produces leachate containing dissolved organic matter, inorganic ions, and potentially toxic constituents, including lead and cadmium [1]. The combination of high rainfall, shallow groundwater use, and permeable near-surface materials makes this process particularly consequential in the Port Harcourt area, within a wider global need for improved municipal-waste management [14].

The local hydrogeological setting increases this vulnerability. The near-surface Benin Formation is dominated by unconsolidated sands and gravels with discontinuous clayey interbeds. These sandy materials support productive groundwater supplies but can also provide pathways for downward and lateral movement of surface-derived contaminants. Many households depend on boreholes for domestic water, so water-quality deterioration near dumpsites can create direct exposure risks. Leachate influence may be indicated by elevated dissolved ions, metals, microbial counts, and a shift from natural recharge chemistry; however, each indicator requires interpretation in its geological context [1], [2].

Electrical-resistivity methods provide a non-invasive means of mapping subsurface contrasts associated with waste disposal. Vertical electrical sounding (VES) resolves the variation of apparent resistivity with depth, whereas electrical resistivity tomography (ERT) provides two-dimensional images of lateral and vertical resistivity variation [19], [20]. Conductive zones beneath or adjacent to dumpsites can be consistent with leachate-affected materials because dissolved ions increase pore-fluid conductivity. This interpretation is nevertheless non-unique: clay-rich strata, high saturation, and naturally mineralised groundwater can also produce low resistivity. Geophysical observations should therefore be assessed together with hydrochemical evidence and the protective character of the overburden rather than treated as independent chemical proof of contamination [3], [4], [29].

Previous investigations in Port Harcourt have demonstrated both the utility and the limits of resistivity-based dumpsite assessment. Integrated VES, ERT, and groundwater-quality data have identified low-resistivity zones, weak overburden protection, and water-quality departures around urban dumpsites [3]. Other local studies have mapped shallow conductive anomalies or lateral plume migration but have not always paired those observations with sufficient hydrochemical validation or aquifer-protective-capacity assessment [4], [6]. Recent Nigerian studies similarly show the value of integrating resistivity imaging with water chemistry and health-risk indicators [23], [24], [25]. Consequently, the degree to which conductive subsurface anomalies correspond with groundwater deterioration remains site dependent.

This article assesses groundwater quality near urban dumpsites at Eliozu, Rumuolumeni, and Iwofe in Port Harcourt using integrated VES, ERT, and borehole hydrochemical data. Seventeen VES stations and thirteen ERT profiles were used to examine subsurface resistivity structure, conductive anomalies, and geoelectric protective capacity. Six borehole samples—three collected close to dumpsites and three at more distant comparison locations—were assessed using physicochemical, microbial, heavy-metal, groundwater-quality-index (GQI), and hydrochemical-facies indicators. The analysis examines whether conductive anomalies and weak geoelectric protection co-occur with poorer measured water quality at the sampled locations; it does not establish source-specific contaminant transport from a single sampling campaign.

Leachate migration from municipal solid waste is governed by waste composition, moisture conditions, landfill age, and the hydrogeological properties of the receiving environment. Landfill leachate may contain substantial concentrations of dissolved salts, organic matter, ammoniacal nitrogen, chloride, and metals, although composition changes as waste decomposes and as the plume interacts with aquifer materials [1]. For this reason, neither a single chemical parameter nor a low-resistivity anomaly alone can establish the source, geometry, or groundwater impact of a plume. Integrated geophysical and hydrochemical assessment is most useful where it distinguishes conductive waste-affected materials from naturally conductive lithologies and relates those materials to measured water quality.

Electrical-resistivity surveys have been widely applied to this problem because they provide spatial coverage that borehole sampling alone cannot supply. VES is suited to estimating the depth, thickness, and resistivity of layered subsurface units, while ERT can reveal changes in the lateral continuity and vertical extent of conductive zones. Recent ERT applications confirm its usefulness for landfill characterisation and monitoring, while also reinforcing the need for site-specific hydrogeological control [26], [27], [28], [30]. An integrated Port Harcourt study [3] reported low-resistivity zones interpreted as leachate-affected materials, high-resistivity zones associated with landfill gas, weak overburden protection, and groundwater parameters that departed from drinking-water guidelines. This evidence illustrates the value of combining geoelectric and hydrochemical observations, but it also demonstrates that plume interpretation depends on the local sequence of clay, fine sand, coarse sand, and gravel.

An earlier Port Harcourt landfill assessment combined two-dimensional resistivity imaging with physicochemical and microbial water analyses [5]. It linked conductive subsurface zones, low pH, and elevated microbial counts, illustrating the value of evaluating geophysical anomalies with direct water-quality indicators. Its single-time survey design did not resolve seasonal changes in migration or aquifer response, a limitation that also applies to many site-specific dumpsite investigations.

Several studies have focused primarily on resistivity evidence. A survey at Eneka, Rivers State [4], used Wenner and Schlumberger measurements to distinguish low-, intermediate-, and high-resistivity zones. The low-resistivity zones were interpreted as leachate and landfill-gas effects extending to approximately 14 m depth and laterally from the dumpsite. At an Obigbo dumpsite, VES data identified vertical and lateral movement of conductive contaminants to about 15.6 m depth [6]. The deeper aquifer remained protected by intervening clay, showing why depth to aquifer and overburden composition are essential to risk interpretation. These studies establish the capacity of resistivity methods to delineate anomalous zones, but they do not independently establish the chemical condition of groundwater at every anomalous location.

At Eligbolo–Eliozu, two-dimensional resistivity imaging identified shallow and laterally migrating low-resistivity zones interpreted as leachate and gas migration toward the groundwater system [7]. This result is particularly relevant to the Eliozu component of the present work because it demonstrates local variation in migration pathways around an urban dumpsite. Across Nigerian settings, combined geophysical and geochemical assessment has also provided a stronger environmental interpretation than either evidence stream in isolation [8]. A recent review of Nigerian dumpsite studies likewise identified the need to relate leachate indicators to local groundwater quality rather than generalise from resistivity alone [2].

The unresolved issue is not whether dumpsites can produce conductive anomalies, but whether those anomalies co-occur with poorer sampled groundwater quality and weak geoelectric protection at comparable locations. The present study addresses this issue by combining VES- and ERT-derived evidence with Dar Zarrouk parameters and paired near-dumpsite/comparison borehole analyses at three Port Harcourt dumpsites. Its contribution is regional and comparative: it evaluates these evidence streams within the same cross-sectional assessment. The field data represent conditions only at the sampled locations and time of investigation and cannot, on their own, identify a unique contaminant source.

2. Materials and Methods

The investigation covered three urban dumpsite environments at Eliozu, Rumuolumeni, and Iwofe in Port Harcourt, Rivers State, Nigeria. The sites lie within the Niger Delta sedimentary basin,

where the near-surface Benin Formation comprises predominantly unconsolidated sands and gravels with discontinuous clayey interbeds. Reconnaissance established survey locations from waste-deposit positions, drainage features, surface depressions, access conditions, and nearby boreholes. Stations were placed to represent each dumpsite setting while avoiding major sources of electrical interference, including power infrastructure, metallic fencing, pipelines, and reinforced structures. Geographic positions and coordinates were recorded and verified borehole-locations were identified.

The VES design comprised six stations at Iwofe (VES 1–6), five at Rumuolumeni (VES 7–11), and six at Eliozu (VES 12–17). The corresponding full current-electrode spreads were 100 m at Iwofe and 80 m at Rumuolumeni and Eliozu. ERT coverage comprised five 100-m profiles at Iwofe (ERT 1–5), four 150-m profiles at Rumuolumeni (ERT 6–9), and four 150-m profiles at Eliozu (ERT 10–13). Iwofe and Rumuolumeni profiles were oriented principally east–west, with one north–south line at each site; Eliozu profiles followed northwest–southeast, southwest–northeast, and northeast–southwest orientations. This layout provides local two-dimensional sections but does not constitute a three-dimensional plume model.

Geoelectrical data were acquired with an ABEM Terrameter SAS 1000, stainless-steel electrodes, insulated cables, measuring tapes, and a Garmin 60 GPS receiver. VES used the Schlumberger array and ERT used the Wenner array. For VES, current-electrode spacing was progressively expanded while potential electrodes remained near the sounding centre and were expanded only when the potential difference became too small for reliable measurement. Electrode contact, cable continuity, alignment, and the absence of nearby conductive infrastructure were checked during acquisition. Where dry ground affected contact, water was applied locally around the electrodes. The acquisition system and field controls followed the operational guidance for the Terrameter SAS series [9].

For each VES measurement, apparent resistivity was obtained from the measured potential difference and injected current:

$$\rho_a = K\frac{\Delta V}{I},$$

where ρ_a is apparent resistivity ($\Omega\, m$), K is the array geometric factor, ΔV is the measured potential difference, and I is current. VES curves were inspected on logarithmic plots and inverted with IPI2Win using one-dimensional least-squares forward modelling. Layer resistivity, thickness, and depth were obtained from the inverted models. ERT data were inverted in RES2DINV to produce measured and calculated apparent-resistivity pseudosections and inverse-model resistivity sections. The reported VES misfits were generally below 10%. Low-resistivity zones were described first as conductive anomalies and interpreted as potentially leachate-affected in conjunction with site setting, existing lithological data, and water-quality observations. This distinction avoids treating electrical conductivity as direct chemical confirmation.

Aquifer protective capacity was evaluated from Dar Zarrouk parameters derived from the VES layer models. For layers above the aquifer, transverse resistance (T) and longitudinal conductance (S) were calculated as:

$$T = \sum_{i=1}^{n} \rho_i h_i, \qquad S = \sum_{i=1}^{n} \frac{h_i}{\rho_i},$$

where ρ_i and h_i are the resistivity and thickness of layer i. Longitudinal conductance is particularly relevant because electrically conductive, clay-rich overburden can retard the vertical movement of

contaminants. The reported values were classified using the modified longitudinal-unit-conductance scheme, in which $S < 0.10$ S denotes poor protective capacity [10], [11].

Six groundwater samples were collected from functional boreholes reported as 20–100 m deep. BH1, BH3, and BH5 represented locations close to the Eliozu, Rumuolumeni, and Iwofe dumpsites, respectively, while BH2, BH4, and BH6 were more distant comparison locations. Boreholes were pumped for at least five minutes before collection. Samples were collected in pre-acid-washed 1 L high-density polyethylene bottles, stored below 4 °C, and transported for laboratory analysis. In-situ measurements included pH, temperature, electrical conductivity, salinity, turbidity, and total dissolved solids using a Hanna HI9829 multiparameter meter; temperature was cross-checked with a mercury-filled thermometer. Laboratory analyses determined phosphate, nitrate, sulphate, chloride, total alkalinity, total hardness, bicarbonate, calcium, magnesium, sodium, potassium, iron, lead, and cadmium. Iron, lead, and cadmium were measured with a TECHCOMP AA6000 atomic-absorption spectrophotometer; bicarbonate, sodium, and potassium were derived from the reported hydrochemical dataset. Total heterotrophic bacteria were enumerated by standard plate count, while total and faecal coliforms were determined by the multiple-tube fermentation method. Sample handling and laboratory procedures followed Standard Methods and recognised water-sampling guidance [12], [16], [17], [18].

Analytical consistency of the major-ion data was examined using cation–anion balance error (CBE):

$$CBE(\%) = \frac{\sum cations - \sum anions}{\sum cations + \sum anions} \times 100.$$

Groundwater quality was summarised with the weighted-arithmetic GQI. For each selected parameter, a relative weight was applied to a quality rating based on the measured concentration, the relevant drinking-water standard, and the ideal value. The quality rating (q_i), sub-index (SI_i), and overall index were calculated as:

$$q_i = \frac{C_i - V_i}{S_i - V_i} \times 100, \qquad SI_i = W_i q_i, \qquad GQI = \sum_i SI_i,$$

where C_i is the measured concentration, S_i is the selected standard, V_i is the ideal value (zero for most parameters and 7 for pH), and W_i is the relative parameter weight. The reported GQI classes were <50, 50–100, 100–200, 200–300, and >300 for excellent, good, poor, very poor, and unsuitable water, respectively [13]. The original dataset preserves the resulting sub-indices and total GQI values but not the individual parameter weights; GQI is therefore used here as a reported comparative index rather than an independently recalculated regulatory-compliance metric. Piper, Gibbs, and Schoeller diagrams were used to characterise groundwater facies and major-ion processes [21], [22], [31], [32], [33]. CBE calculations used major-ion concentrations converted to milliequivalents per litre. Parameter-specific comparisons used the WHO drinking-water guideline framework [15], while the chemical species and units reported by the original laboratory dataset are retained without conversion. The geophysical, protective-capacity, and hydrochemical outputs were then interpreted together as co-occurring evidence of leachate presence.

3. Results

The results combine 17 one-dimensional VES models, 13 two-dimensional ERT profiles, and six borehole-water analyses. VES inversion provided layer resistivity, thickness, and depth, ERT provided two-dimensional resistivity images, and the overburden models provided longitudinal conductance values for aquifer-protective-capacity assessment. Borehole analyses were compared

between three dumpsite-proximal locations (BH1, BH3, and BH5) and the corresponding controls (BH2, BH4, and BH6). The evidence is interpreted as a comparative assessment of the sampled locations; it does not establish temporal changes in plume extent or groundwater quality.

3.1 Geoelectric Evidence of Conductive Zones

The VES models show heterogeneous sandy, silty, and weathered subsurface materials at the three dumpsite environments, with discrete conductive intervals occurring at shallow to intermediate depths. At Iwofe, VES 1 contained conductive layers from 4.63 to 33.20 m, while VES 5 contained a conductive interval from 11.10 to 33.40 m. At Rumuolumeni, VES 7 contained conductive layers from 5.25 to 19.30 m, and VES 8–10 contained shallower conductive zones. At Eliozu, conductive intervals were identified in VES 12–16; VES 13 and VES 14 contained the lowest reported resistivities, with conductive layers extending from 1.52 to 21.80 m and from 1.79 to 22.60 m, respectively. These patterns identify zones that are consistent with potential leachate-affected materials in the context of the dumpsite settings and the subsequent water-quality evidence.

The ERT inverse sections provide lateral context that cannot be obtained from individual soundings. The representative sections at Iwofe, Rumuolumeni, and Eliozu display shallow to intermediate conductive zones within weathered and sandy materials. At Iwofe, the image indicates conductive material extending through weathered sandy units; at Rumuolumeni, low-resistivity zones occur in parts of the shallow profile, particularly between approximately 2 and 10 m; and at Eliozu, conductive zones are more continuous within the weathered overburden. These observations identify possible conductive pathways.

Figure 1: Representative inverse-model resistivity section at Iwofe (ERT 1). Interpretive labels in the source image are not treated as direct chemical confirmation.

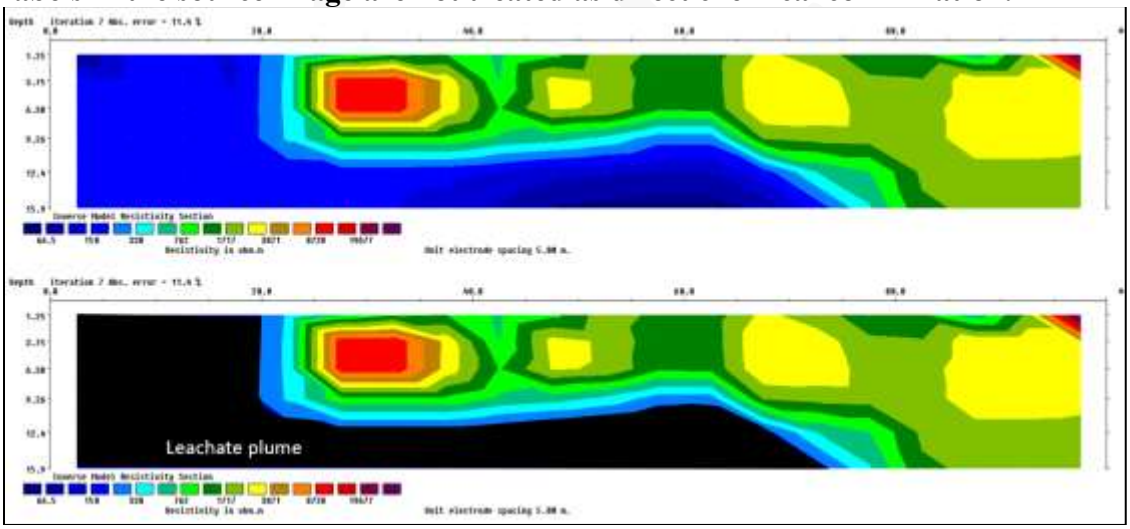


Figure 2: Representative inverse-model resistivity section at Rumuolumeni (ERT 6). Interpretive labels in the source image are not treated as direct chemical confirmation.

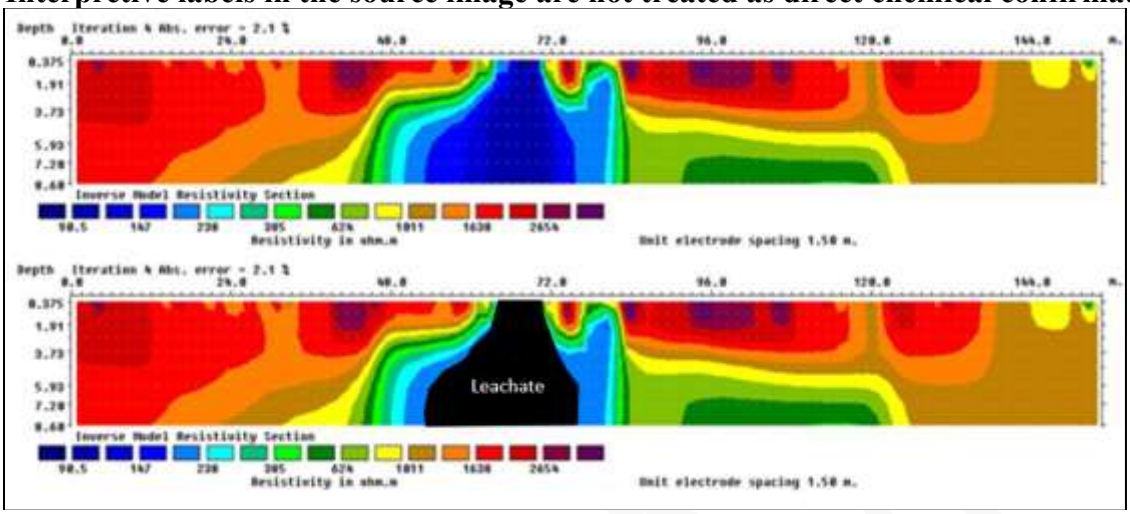
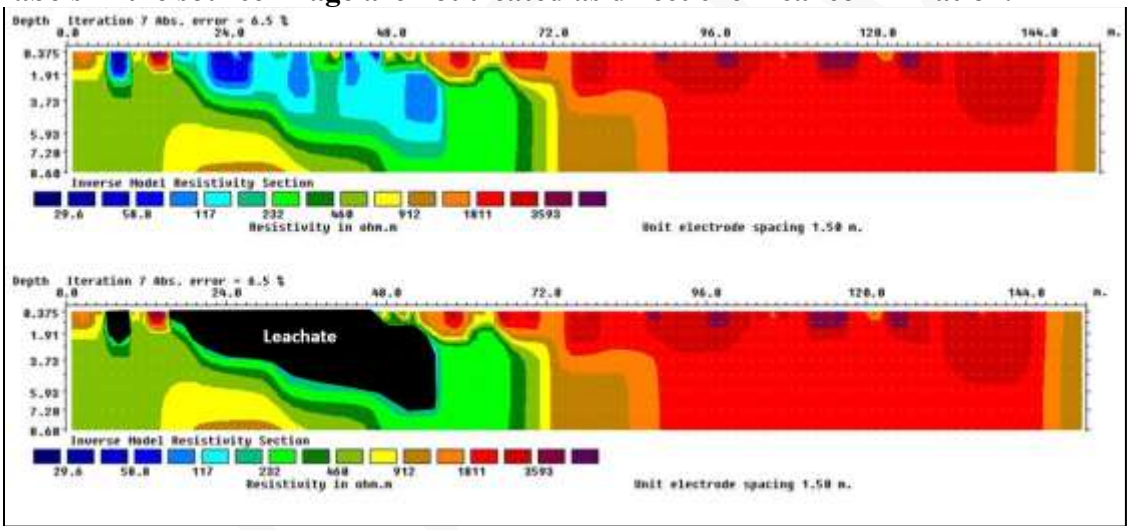


Figure 3: Representative inverse-model resistivity section at Eliozu (ERT 10). Interpretive labels in the source image are not treated as direct chemical confirmation.



3.2 Aquifer Protective Capacity

Longitudinal conductance across the 17 VES stations ranged from 0.001877 to 0.023766 S. Every value is below the 0.10 S threshold for poor protective capacity. The largest value, 0.023766 S at VES 7 in Rumuolumeni, remains within the poor class, while the lowest value, 0.001877 S at VES 17 in Eliozu, indicates limited capacity for the overburden to retard downward contaminant movement. The result is consistent with the predominance of permeable sandy and weathered materials in the near-surface sequence.

The protective-capacity result is important to the geoelectric interpretation. Conductive zones beneath dumpsites identify possible conductive pathways, while low longitudinal conductance places the overburden in the poor class of the adopted geoelectric scheme. Accordingly, the evidence is most suggestive where a conductive anomaly, a poor classification, and poorer measured water quality co-occur.

Table 1: Derived Dar Zarrouk parameters and reported geoelectric protective-capacity classification.

VES	Location	Transverse resistance (Ω m²)	Longitudinal conductance (S)	Reported class
1	Iwofe	241591.20	0.004576	Poor
2	Iwofe	195580.50	0.005748	Poor
3	Iwofe	325044.60	0.003391	Poor
4	Iwofe	253880.40	0.004342	Poor
5	Iwofe	175642.70	0.006323	Poor
6	Iwofe	265592.30	0.003827	Poor
7	Rumuolumeni	154928.20	0.023766	Poor
8	Rumuolumeni	43906.69	0.013010	Poor
9	Rumuolumeni	49211.49	0.010759	Poor
10	Rumuolumeni	27341.32	0.013427	Poor
11	Rumuolumeni	162284.30	0.001883	Poor
12	Eliozu	98107.36	0.002468	Poor
13	Eliozu	25711.90	0.018382	Poor
14	Eliozu	74486.90	0.006845	Poor
15	Eliozu	69461.65	0.005741	Poor
16	Eliozu	63284.10	0.005514	Poor
17	Eliozu	168779.60	0.001877	Poor

The classification follows the adopted modified longitudinal-conductance rating scheme ($S <$ 0.10 S = poor). These values describe geoelectric overburden conditions under that scheme.

3.3 Impacted–Control Groundwater Quality Contrast

The water analyses show a marked contrast between the dumpsite-proximal and control boreholes in the GQI results. BH1, BH3, and BH5 recorded GQI values of 126.72, 163.71, and 198.88, respectively, and were classified as poor quality. BH2, BH4, and BH6 recorded values of 35.94, 36.18, and 36.35, respectively, and were classified as excellent quality. BH5 at Iwofe had the largest GQI value, followed by BH3 at Rumuolumeni and BH1 at Eliozu. The contrast is driven principally by higher phosphate, nitrate, iron, lead, cadmium, magnesium, and chloride contributions in the impacted samples.

Table 2: Groundwater Quality Index results for impacted and control boreholes.

Dumpsite environment	Impacted borehole	GQI	Classification	Control borehole	GQI	Classification
Eliozu	BH1	126.72	Poor quality	BH2	35.94	Excellent quality
Rumuolumeni	BH3	163.71	Poor quality	BH4	36.18	Excellent quality
Iwofe	BH5	198.88	Poor quality	BH6	36.35	Excellent quality

Individual parameters support this descriptive contrast (Table 3). Relative to the comparison boreholes, the near-dumpsite samples contained higher phosphate (1.2–2.5 mg/L), nitrate reported as NO_3^- (15–35 mg/L), iron (0.8–1.8 mg/L), and cadmium (0.0010–0.0034 mg/L). The laboratory dataset used 10 mg/L as its nitrate comparison value. The pH values of all six samples were below

the reported 6.5–8.5 range, including the comparison boreholes. Thus, the excellent GQI classifications of BH2, BH4, and BH6 are relative composite-index results, not evidence that every individual parameter satisfies a drinking-water reference value. Lead was 0.01–0.02 mg/L in the near-dumpsite samples and reported as <0.01 mg/L in comparison samples

Table 3: Reported physicochemical, major-ion, microbial, and Heavy-metal results for the six sampled boreholes.
BH1/BH2, BH3/BH4, and BH5/BH6 are the Eliozu, Rumuolumeni, and Iwofe near-dumpsite/comparison pairs, respectively

S/N	Parameters	Method	BH1 (Eliozu Impacted)	BH2 (Eliozu Control)	BH3 (Rumuolumini Impacted)	BH4 (Rumuolumini Control)	BH5 (Iwofe Impacted)	BH6 (Iwofe Control)	WHO Standard
1	pH	APHA4500HB	5.5	4.8	5.8	5	5.8	4.9	6.5–8.5
2	Appearance	APHA2110	Turbid	Clear	Turbid	Clear	Turbid/Yel.	Clear	Bright/Clear
3	Odor	APHA2110	Objection.	Unobj.	Objection.	Unobj.	Putrid	Unobj.	Unobj.
4	Taste	APHA2110	Objection.	Unobj.	Objection.	Unobj.	Objection.	Unobj.	Unobj.
5	Temperature (∘C)	APHA2550A	30.1	30.1	30.7	31.2	31	30.2	Ambient
6	EC (µS/cm)	APHA2510B	100	45	210	55	103	62	500
7	TDS (ppm)	APHA2130B	149	28	88.6	34	200	39.5	500
8	Total Alk. (mg/L)	APHA2320B	33	4	45	5	70	8	200
9	Bicarbonate (HCO3−)	Calculated	40	5	55	6	85	10	-
10	Chloride (Cl−)	APHA4500B	72	10	95	12	88	12	250
11	Total Hardness	APHA2340C	78	9	102	12	88	13.5	150
12	Calcium (Ca2+)	APHA3111B	18	2	25	2.5	22	3	70
13	Magnesium (Mg2+)	APHA3111B	8	1	12	1.5	10	1.5	20
14	Sodium (Na+)	Calculated	45	5	32	5	40	7	200
15	Potassium (K+)	Calculated	8	1	6	1.5	8	1.5	-
16	Phosphate (PO43−)	APHA4500PD	1.2	0.05	1.8	0.06	2.5	0.05	0.5
17	Sulphate (SO42−)	APHA4500	25	3	35	4	25	4.5	200
18	Nitrate (NO3−)	APHA4500NO3	15	1	22	1.5	35	1.5	10
19	THB (cfu/mL)	APHA9221E	2.5×10^{2}	1.0×10^{1}	1.2×10^{3}	1.5×10^{1}	1.5×10^{5}	1.2×10^{1}	100
20	TCB (cfu/mL)	APHA9221B	1.2×10^{2}	0	3.5×10^{2}	0	4.5×10^{3}	0	NIL
21	FCB (cfu/mL)	APHA9221E	1.0×10^{1}	0	8.0×10^{1}	0	1.8×10^{2}	0	NIL
22	Iron (Fe) (mg/L)	APHA3111C	0.8	0.02	1.8	0.05	1.2	0.05	0.3
23	Lead (Pb) (mg/L)	APHA3111C	0.02	<0.01	0.01	<0.01	0.01	<0.01	0.01
24	Cadmium (Cd)	APHA3111B	0.0013	<0.001	0.001	<0.001	0.0034	<0.001	0.003

The major-ion balance provides an important qualification to the hydrochemical interpretation (Table 4). BH1, BH2, BH4, and BH6 had reported CBE values within ±5%, which falls within the excellent range of less than 5%. This shows good agreement between the total measured cation and anion, meaning measured dissolved ions were properly accounted for, whereas BH3 (−11.07%) and BH5 (−13.18%) were outside the stated ±10% tolerance, which may be due to analytical error and ot overestimation of anions.

Table 4: Reported cation–anion balance and GQI results.

Borehole	Σ cations (meq/L)	Σ anions (meq/L)	CBE (%)	CBE assessment	GQI	GQI class
BH1	3.719	3.487	3.22	Within ±5%	126.72	Poor
BH2	0.425	0.444	−2.19	Within ±5%	35.94	Excellent
BH3	3.780	4.721	−11.07	Outside ±10%	163.71	Poor
BH4	0.504	0.546	−4.01	Within ±5%	36.18	Excellent
BH5	3.865	5.039	−13.18	Outside ±10%	198.88	Poor
BH6	0.616	0.622	−0.47	Within ±5%	36.35	Excellent

Figure 4: Piper diagram of reported major-ion composition for BH1–BH6.

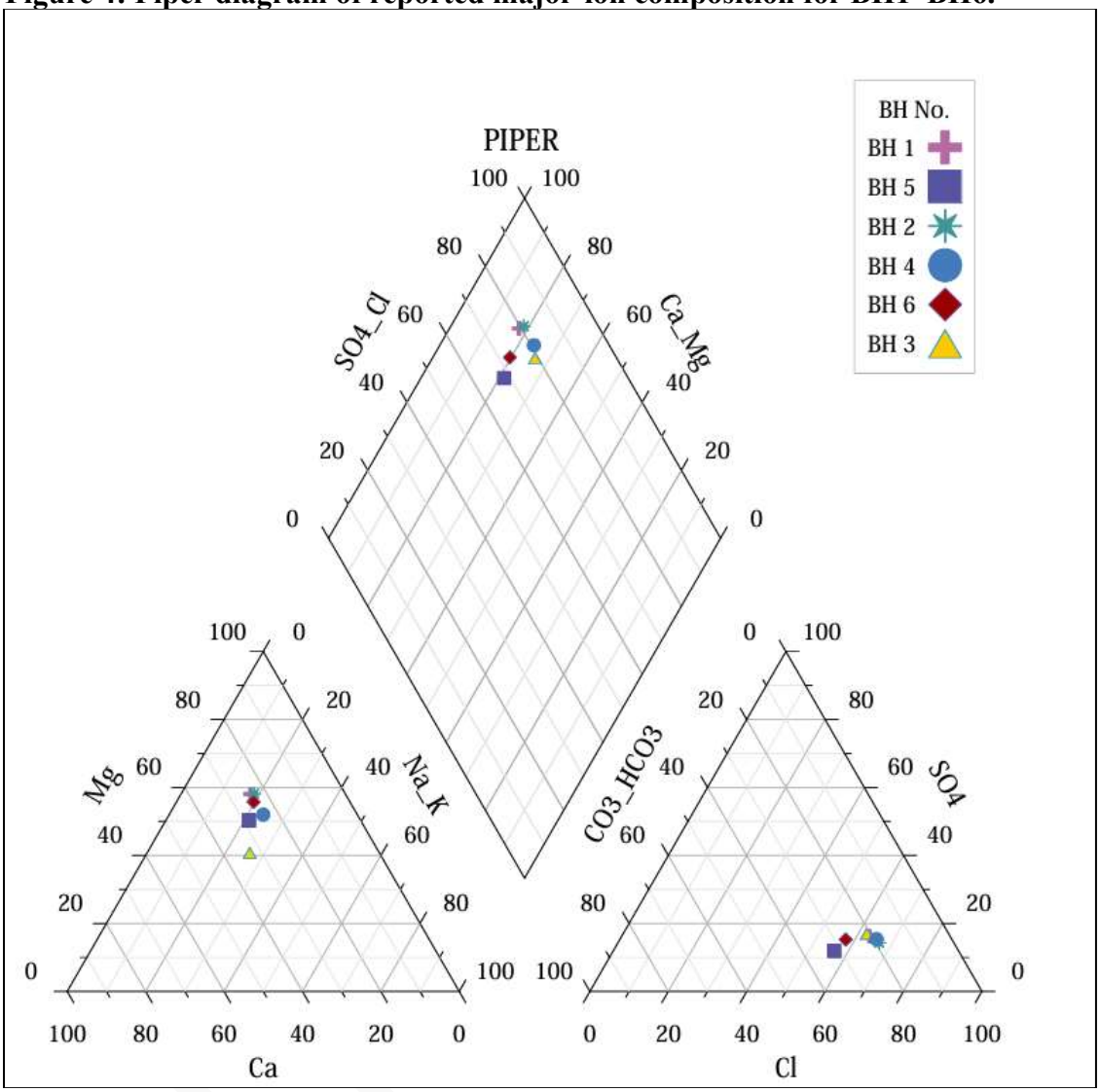


Figure 5: Gibbs cation–anion ratio plots for the reported groundwater samples.

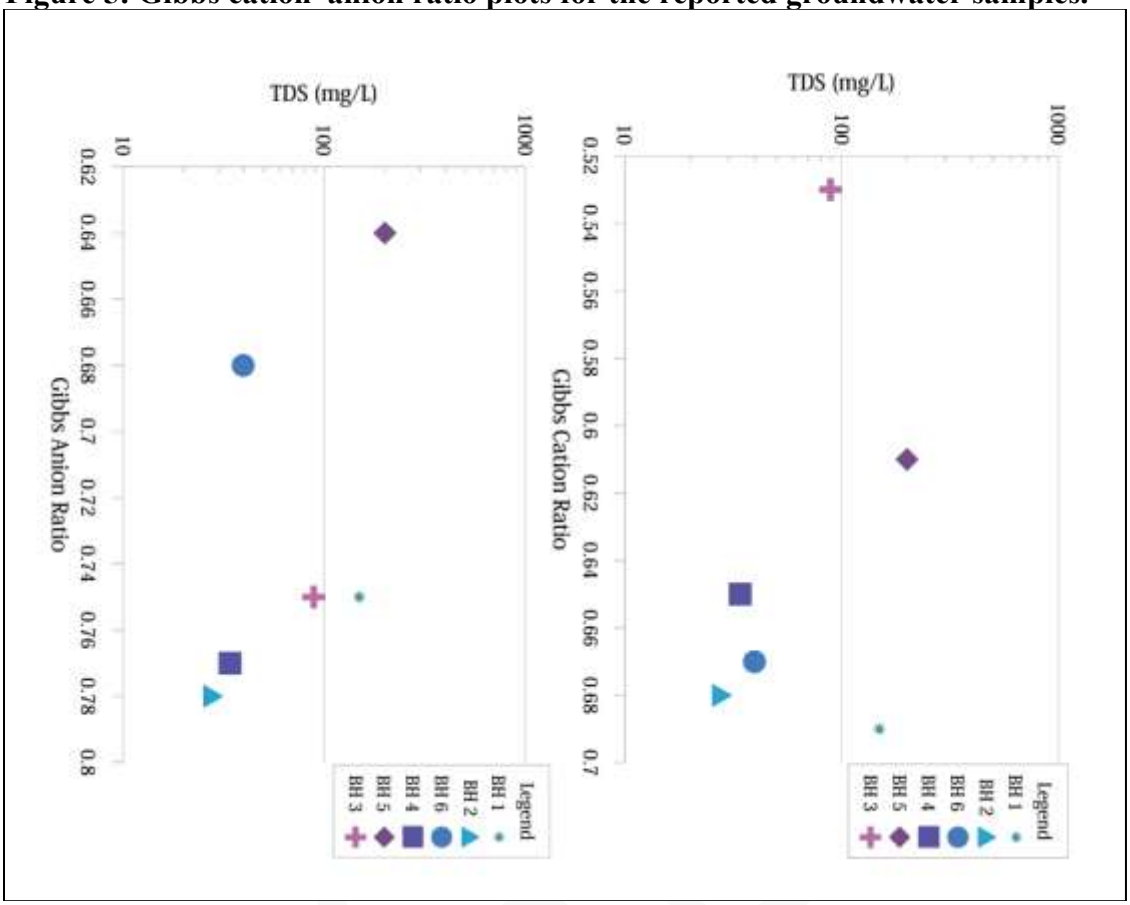
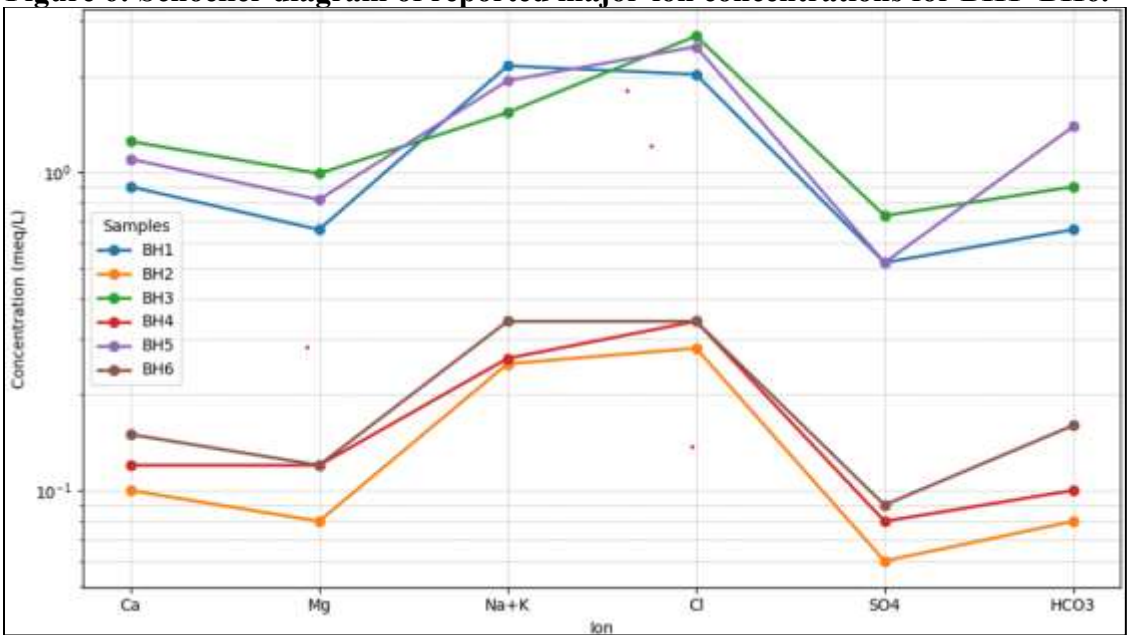


Figure 6: Schoeller diagram of reported major-ion concentrations for BH1–BH6.



4. Discussion

4.1 Hydrochemical Facies and Integrated Interpretation

The Piper, Gibbs, and Schoeller plots provide a descriptive interpretation of the reported major-ion data (Figures 4–6). The Piper plot places the samples toward the alkali-metal and chloride fields, consistent with a Na–K–Cl tendency rather than a calcium–bicarbonate-dominant type. The Gibbs plots place the samples principally within the rock-dominance/water–rock-interaction field. The Schoeller diagram separates BH1, BH3, and BH5 as a higher-concentration group from BH2, BH4, and BH6. This pattern indicates that the groundwater is not mainly a fresh a fresh calcium-bicarbonate type, which is usually expected from recently recharged groundwater. Instead the samples show an alkali-chloride character, meaning that the dominant facies is mainly Na-K-Cl type.

Taken together, the results provide mutually reinforcing but not identical evidence. Conductive zones and poor geoelectric protective-capacity classifications identify subsurface conditions that are more susceptible to surface-derived inputs. The higher reported GQI values and higher phosphate, nitrate, iron, lead, and cadmium concentrations in the near-dumpsite boreholes indicate poorer measured quality at those sampled locations. The Na–K–Cl tendency and chloride enrichment are consistent with water–rock interaction together with possible anthropogenic inputs.

5. Conclusion

This study integrated 17 VES stations, 13 ERT profiles, and six borehole-water analyses to assess groundwater quality near urban dumpsites at Eliozu, Rumuolumeni, and Iwofe in Port Harcourt. The resistivity models identified shallow to intermediate conductive anomalies, including intervals extending to 33.40 m at Iwofe. Longitudinal conductance ranged from 0.001877 to 0.023766 S, placing every investigated VES point in the poor class of the adopted geoelectric protective-capacity rating scheme. The hydrochemical results showed a clear near-dumpsite/comparison contrast: BH1, BH3, and BH5 had reported GQI values of 126.72, 163.71, and 198.88, which are poor, whereas BH2, BH4, and BH6 had values of 35.94, 36.18, and 36.35 which are excellent following the adopted scheme. The reported higher phosphate, nitrate, iron, lead, and cadmium concentrations at near-dumpsite locations and the alkali-chloride tendency are consistent with chemical alteration.

The co-occurrence of conductive anomalies, poor geoelectric protective-capacity classifications, and poorer measured composite water quality justifies confirmatory impacts of leachates infiltration on groundwater around the impacted boreholes locations investigated near dumpsites. The interpretation is bounded by the single sampling campaign and charge-balance errors outside the stated tolerance for BH3 and BH5. Water from the near-dumpsite boreholes should not be relied upon for drinking without confirmatory testing and treatment appropriate to confirmed contaminants.

6. Recommendations

Based on the findings of this study it is recommended that:

I. Considering the geophysical and hydrochemical findings, all boreholes in Eliozu, Rumuolumeni, and Iwofe require comprehensive treatment before domestic use. This includes neutralization of acidity to achieve pH levels within 6.5–8.5, removal of heavy metals with particular focus on lead, and microbial disinfection to eliminate heterotrophic and coliform bacteria.

II. Borehole siting should prioritize areas with moderate-to-good aquifer protective capacity and avoid proximity to dumpsites. Structural safeguards such as reinforced well casings and sanitary seals are essential to prevent further contamination from surface infiltration.
III. Long-term monitoring of hydrochemical and geophysical parameters is critical for tracking leachate migration and assessing aquifer response over time.
IV. Dumpsites should be upgraded with engineered containment structures, including clay liners, geomembranes, and leachate-collection drains, to minimize further leachate percolation.
V. Targeted remediation strategies, including permeable reactive barriers, bioremediation techniques, and advanced physicochemical treatment technologies, should be implemented in high-risk zones, particularly Eliozu and Rumuolumeni. Regulatory enforcement, community engagement, and participatory environmental monitoring are indispensable for sustainable groundwater management.
VI. Incorporation of climate-responsive risk assessments will enhance aquifer resilience against seasonal leachate surges and long-term water quality degradation.
VII. Future work should repeat geophysical and hydrochemical measurements across wet and dry seasons, verify major-ion balance with repeat laboratory analysis, document well construction and groundwater-flow direction, and use additional upgradient and downgradient boreholes to constrain potential transport pathways.

References

[1] Christensen, T. H., Kjeldsen, P., Bjerg, P. L., Jensen, D. L., Christensen, J. B., Baun, A., Albrechtsen, H.-J., & Heron, G. (2001). Biogeochemistry of landfill leachate plumes. *Applied Geochemistry*, 16(7–8), 659–718.

[2] Aladejana, J. A., Adeoti, L., & Ajibade, O. (2021). Leachate impact of solid waste dumpsites on groundwater quality in Nigeria: A review. *Heliyon*, 7(9), e08072.

[3] Agbemuko, O. S., Tamunobereton-Ari, I., & Ngah, S. A. (2017). Determination of the effect of dumpsites on aquifer at Port Harcourt Metropolis, Rivers State, Nigeria. *IOSR Journal of Applied Physics*, 9(6), 41–54.

[4] Nwankwo, C. N., & Ogoro, M. (2020). Geophysical investigation of the impact of solid waste dump on subsurface soil and groundwater in Eneka, Rivers State, Nigeria. *GeoScience Engineering*, 66(3), 121–135.

[5] Ehirim, C. N., Ebeniro, J. O., & Ogwu, D. A. (2009). A geophysical and hydro-physiochemical study of the contaminant impact of a solid waste landfill (SWL) in Port Harcourt Municipality, Nigeria. *Pacific Journal of Science and Technology*, 10(2), 596–603.

[6] Tamuno, W., & Inichinbia, S. (2019). Vertical electric sounding of leachate contaminant plumes at a dumpsite in Obigbo, Rivers State, Nigeria. *Journal of Applied Sciences and Environmental Management*, 23(12), 2245–2249.

[7] Ogbonna, V. A., Nwankwoala, H. O., & Lawal, O. (2017). Impacts of landfill on groundwater quality in Eligbolo-Eliozu, Obio/Akpor Local Government Area, Rivers State, Nigeria. *International Journal of Emerging Engineering Research and Technology*, 5(1), 20–27.

[8] Ayolabi, E. A., Folorunso, A. F., & Kayode, O. T. (2013). Integrated geophysical and geochemical methods for environmental assessment of a municipal dumpsite in Lagos, Nigeria. *Journal of Applied Sciences and Environmental Management*, 17(4), 503–507.

[9] ABEM Instrument. (2010). *ABEM instruction manual: Terrameter SAS 4000 / SAS 1000*.

[10] Oladapo, M. I., Akintorinwa, O. J., & Olorunfemi, M. O. (2004). Geoelectric investigation of the Ondo State Housing Corporation Estate, Nigeria. *Journal of Mining and Geology*, 40(1), 41–48.

[11] Ibanga, J. I., & George, N. J. (2016). Estimating geohydraulic parameters, protective strength, and corrosivity of hydrogeological units: A case study of ALSCON, Ikot Abasi, Southern Nigeria. *Arabian Journal of Geosciences*, 9, 363.

[12] American Public Health Association, American Water Works Association, & Water Environment Federation. (2005). *Standard methods for the examination of water and wastewater* (21st ed.). American Public Health Association.

[13] Patel, D. D., et al. (2023). Application of the Weighted Arithmetic Water Quality Index method for groundwater assessment. *Water*, 15(19), 3512.

[14] United Nations Environment Programme, & International Solid Waste Association. (2024). *Global Waste Management Outlook 2024: Beyond an age of waste—Turning rubbish into a resource*. United Nations Environment Programme. https://doi.org/10.59117/20.500.11822/44939

[15] World Health Organization. (2022). *Guidelines for drinking-water quality: Fourth edition incorporating the first and second addenda*. World Health Organization. https://www.who.int/publications/i/item/9789240045064

[16] American Public Health Association, American Water Works Association, & Water Environment Federation. (2023). *Standard methods for the examination of water and wastewater* (24th ed.). APHA Press.

[17] International Organization for Standardization. (2018). *ISO 5667-3:2018: Water quality—Sampling—Part 3: Preservation and handling of water samples*. ISO.
[18] U.S. Environmental Protection Agency. (2002). *Ground-water sampling guidelines for Superfund and RCRA project managers*. EPA 542-S-02-001. U.S. Environmental Protection Agency.
[19] Loke, M. H. (2014). *Tutorial: 2-D and 3-D electrical imaging surveys*. Geotomo Software.
[20] Dahlin, T., & Zhou, B. (2004). A numerical comparison of 2D resistivity imaging with 10 electrode arrays. *Geophysical Prospecting*, 52(5), 379–398. https://doi.org/10.1111/j.1365-2478.2004.00423.x
[21] Appelo, C. A. J., & Postma, D. (2005). *Geochemistry, groundwater and pollution* (2nd ed.). A.A. Balkema.
[22] Fetter, C. W. (2018). *Applied hydrogeology* (4th ed.). Waveland Press.
[23] Alao, J. O., Lawal, H. A., & Shettima, N. M. (2023). Investigation of groundwater vulnerability to open dumpsites and its potential risk using electrical resistivity and water analysis. *Heliyon*, 9(2), e13265. https://doi.org/10.1016/j.heliyon.2023.e13265
[24] Alao, J. O., Fahad, A., Abdo, H. G., Ayejoto, D. A., Almohamad, H., Ahmad, M. S., Nur, M. S., Danjuma, T. T., Yusuf, M. A., Francis, O. T., & Joy, A. O. (2023). Effects of dumpsite leachate plumes on surface and groundwater and the possible public health risks. *Science of the Total Environment*, 897, 165469. https://doi.org/10.1016/j.scitotenv.2023.165469
[25] Badmus, G. O., Ogungbemi, O. S., Enuiyin, O. V., Adeyeye, J. A., & Ogunyemi, A. T. (2022). Delineation of leachate plume migration and appraisal of heavy metals in groundwater around Emirin dumpsite, Ado-Ekiti, Nigeria. *Scientific African*, 17, e01308. https://doi.org/10.1016/j.sciaf.2022.e01308
[26] Alao, J. O., Otorkpa, O. J., Abubakar, F., Eshimiakhe, D., Aliyu, A., Abdulsalami, M., & Abdulmalik, D. O. (2024). Geoelectrical resistivity and geochemistry monitoring of landfill leachates due to the seasonal variations and the implications on groundwater systems and public health. *Scientific Reports*, 14, 26542. https://doi.org/10.1038/s41598-024-77727-6
[27] Zaini, M. S. I., & Hasan, M. (2024). Application of electrical resistivity tomography in landfill leachate detection assessment. In A. Anouzla & S. Souabi (Eds.), *A review of landfill leachate: Characterization, leachate environment impacts and sustainable treatment methods* (pp. 1–22). Springer. https://doi.org/10.1007/978-3-031-55513-8_1
[28] Godio, A., & Chiampo, F. (2023). Geophysical monitoring of leachate injection in pretreated waste landfill. *Applied Sciences*, 13(9), 5661. https://doi.org/10.3390/app13095661
[29] May, M. T., Brackman, T. B., May, E. C., & Edwards, W. T. (2024). Use of electrical resistivity tomography to reduce landfill siting risks in the south-central Kentucky karst. *Environmental Earth Sciences*, 83, 688. https://doi.org/10.1007/s12665-024-11984-6
[30] Moraes, B. Y. M. de, Xavier, F. V., Fachin, S. J. da S., & Netto, L. G. (2023). Application of electrical resistivity tomography for subsurface investigation of a dump in the city of Jaciara-MT. *Geologia USP. Série Científica*, 23(4). https://doi.org/10.11606/issn.2316-9095.v23-206488
[31] Piper, A. M. (1944). A graphic procedure in the geochemical interpretation of water-analyses. *Transactions, American Geophysical Union*, 25(6), 914–928. https://doi.org/10.1029/TR025i006p00914
[32] Gibbs, R. J. (1970). Mechanisms controlling world water chemistry. *Science*, 170(3962), 1088–1090. https://doi.org/10.1126/science.170.3962.1088

[33] Schoeller, H. (1962). *Les eaux souterraines: Hydrologie dynamique et chimique, recherche, exploitation et évaluation des ressources*. Masson et Cie.

IJGEM